

1 **Discovery of Clioquinol and Analogues as Novel Inhibitors of Severe Acute Respiratory**
2 **Syndrome Coronavirus 2 Infection, ACE2 and ACE2 - Spike Protein Interaction *In Vitro*.**

3

4 Omonike A. Olaleye*, Manvir Kaur, Collins Onyenaka, Tolu Adebusuyi

5 Department of Pharmaceutical and Environmental Health Sciences, College of Pharmacy and
6 Health Sciences, Texas Southern University, 3100 Cleburne St, Houston, TX 77004

7 *Corresponding author:

8 E-mail address: Omonike.olaleye@tsu.edu (Olaleye, OA)

9 College of Pharmacy and Health Sciences, Texas Southern University, GH 125 Houston, TX
10 77004, USA. Tel.: 713-313-7812

11

12

13

14

15

16

17

18

19

20

21

22

23

24

25

26 **Abstract**

27 Severe Acute Respiratory Syndrome Coronavirus 2 (SARS-CoV-2), the etiological agent for
28 coronavirus disease 2019 (COVID-19), has emerged as an ongoing global pandemic. Presently,
29 there are no clinically approved vaccines nor drugs for COVID-19. Hence, there is an urgent
30 need to accelerate the development of effective antivirals. Here in, we discovered Clioquinol (5-
31 chloro-7-iodo-8-quinolinol (CLQ)), a FDA approved drug and two of its analogues (7-bromo-5-
32 chloro-8-hydroxyquinoline (CLBQ14); and 5, 7-Dichloro-8-hydroxyquinoline (CLCQ)) as potent
33 inhibitors of SARS-CoV-2 infection induced cytopathic effect *in vitro*. In addition, all three
34 compounds showed potent anti-exopeptidase activity against recombinant human angiotensin
35 converting enzyme 2 (rhACE2) and inhibited the binding of rhACE2 with SARS-CoV-2 Spike
36 (RBD) protein. CLQ displayed the highest potency in the low micromolar range, with its antiviral
37 activity showing strong correlation with inhibition of rhACE2 and rhACE2-RBD interaction.
38 Altogether, our findings provide a new mode of action and molecular target for CLQ and
39 validates this pharmacophore as a promising lead series for clinical development of potential
40 therapeutics for COVID-19.

41

42

43

44

45

46

47

48

49

50

51

52

53 **Introduction**

54 Severe Acute Respiratory Syndrome Coronavirus 2 (SARS-CoV-2), a novel RNA
55 betacoronavirus, is the causative agent for coronavirus disease 2019 (COVID-19), which has
56 emerged as an ongoing global pandemic¹. Worldwide, SARS-CoV-2 has spread rampantly to
57 more than 188 countries/regions and has resulted in 18,847,261 confirmed cases, 11,390,018
58 recovered, including 708,540 deaths (<https://coronavirus.jhu.edu/map.html>). Within the United
59 States alone, there are more than 4,825,742 cases, 1,577,851 recovered and a total of 158,300
60 deaths as of August 6th, 2020 according to the Johns Hopkins COVID-19 dashboard. About
61 80% of people infected with SARS-CoV-2 experience mild symptoms or are asymptomatic²;
62 while a majority of symptomatic patients with moderate to severe symptoms have shown a
63 broad range of clinical manifestation and/or significant complications, including severe
64 pneumonia, multi-organ failure, acute cardiac injury, neurological damage, septic shock, acute
65 respiratory distress syndrome (ARDS)³⁻⁶. Recent reports revealed that, individuals with pre-
66 existing medical conditions have increased risk of COVID-19 related morbidity and mortality⁷.
67 Currently, there are no U.S. Food and Drug Administration (FDA) approved drugs for the
68 treatment of COVID-19; but several studies are investigating the potential utility of repurposing
69 clinically approved drugs as treatment options for COVID-19⁸⁻¹². To date, only Remdesivir, an
70 inhibitor of RNA dependent RNA Polymerase has been granted emergency use authorization
71 (EUA) for the treatment of hospitalized patients with severe cases of COVID-19¹³.

72 Historically, Clioquinol (5-chloro-7-iodo-8-quinolinol (CLQ)) and its derivatives belonging
73 to the 8-hydroxyquinoline structural class, has shown potent broad-spectrum activity against
74 clinically relevant pathogens¹⁴⁻²⁰. More recently, CLQ and its analogues have been extensively
75 investigated as potential treatments for cancer and neurodegenerative diseases²¹⁻²⁸. Additional
76 studies have also shown the involvement of CLQ in the efflux mechanisms of ATP binding
77 cassette (ABC) transporters^{29,30} and the cellular autophagic pathway^{31,32}, a critical process in the

78 host defense machinery against viral infections³³. Furthermore, using a high-throughput screen
79 (HTS) and chemical genomics approach, Olaleye, O., et. al. identified and characterized CLQ
80 and certain analogues as potent inhibitors of methionine aminopeptidase¹⁷, a universally
81 conserved metalloprotease required for N-terminal methionine excision^{34,35}. As an established
82 metal chelator and zinc ionophore, CLQ modulates underlying molecular and physiologic
83 machinery required for metal homeostasis^{31, 32, 36-39}. Altogether, these pharmacologic properties
84 of CLQ, makes it an attractive drug for potential targeting of Angiotensin Converting Enzyme 2
85 (ACE2).

86 ACE2 is a zinc metalloprotease and essential cellular receptor for SARS-CoV-2 entry
87 into host cells⁴⁰⁻⁴³. Therefore, rapid identification of potent and selective ACE2 inhibitors have
88 the prospects of accelerating the clinical development of preventative interventions and/or
89 treatment options for COVID-19. ACE2 is mainly expressed in alveolar epithelial cells of the
90 lungs, heart, kidney, and gastrointestinal tract^{44,45}. Although, ACE2 is the cellular receptor for
91 SARS-CoV-2⁴⁰⁻⁴³, ACE2 primarily functions as a carboxypeptidase that catalyzes the
92 conversion of a single residue from angiotensin (Ang II), generating L-phenylalanine and Ang
93 (1-7), a potent vasodilator, thus playing a critical role in controlling hypertension, renal disease,
94 cardiac function and lung injury^{46,47}. The crystalline structure of the ACE2 shows two domains; a
95 N-terminal zinc metallopeptidase domain (MPD) capable of binding the viral envelope-anchored
96 Spike (S) glycoprotein of coronaviruses, and a C terminal “collectrin-like” domain⁴⁸⁻⁵⁰. The
97 interaction of the MPD of ACE2 and S glycoprotein of SARS-CoV-2 is the initial and critical step
98 in viral infection by receptor recognition and fusion of host and viral cellular membranes⁴⁰⁻⁴³. In
99 addition, viral entry requires priming of S protein by a host protease into S1 and S2 subunits,
100 which are responsible for receptor attachment and membrane fusion, respectively⁵¹⁻⁵⁴. A
101 receptor-binding domain (RBD) of the S1 subunit specifically recognizes ACE2 on human
102 cells⁴⁰⁻⁴³. Binding of the S1 subunit to ACE2 receptor triggers a conformational change in S
103 glycoprotein from metastable pre-fusion state to stable post-fusion conformation, resulting in

104 shedding of S1 and transition of the S2 subunit to expose a hydrophobic fusion peptide^{42,55,56}.
105 The initial priming at S1/S2 boundary promotes subsequent cleavage at the S2 site by host
106 proteases, which is critical for membrane fusion and viral infectivity^{54,57,58}. Therefore, targeting
107 the interaction between human ACE2 receptor and the RBD in S protein of SARS-CoV-2 could
108 serve as a promising approach for the development of effective entry inhibitors for potential
109 prevention and/or treatment of COVID-19.

110 In this study, we evaluated the effect of CLQ, and two of its analogues (7-bromo-5-
111 chloro-8-hydroxyquinoline (CLBQ14); and 5, 7-Dichloro-8-hydroxyquinoline (CLCQ)) on SARS-
112 CoV-2 infection induced cytopathic effect (CPE) *in vitro*. In addition, we assessed the
113 cytotoxicity of these compounds. Furthermore, we determined the impact of all three
114 compounds on recombinant human ACE2 (rhACE2) interaction with the RBD on Spike protein
115 of SARS-CoV-2; and independently assessed their effects on the exopeptidase activity of
116 rhACE2. Here in, we discovered for the first time that CLQ, CLBQ14 and CLCQ effectively
117 inhibits the novel SARS-CoV-2 infection induced CPE *in vitro*, inhibited rhACE2 and its
118 interaction with Spike protein and rhACE2 exopeptidase activity in the low micromolar range.
119 Thus, rapid optimization and pre-clinical development of CLQ and its congeners could
120 potentially accelerate their consideration for re-purposing as potential antiviral agents against
121 COVID19, first in non-human primate (NHP) models of SARS-CoV-2 infection, and
122 subsequently in clinical trials.

123

124 **MATERIALS AND METHODS**

125 **MATERIALS**

126 **Cell Growth Conditions and Medium**

127 African Green Monkey Kidney Vero E6 cells (ATCC# CRL-1586, American Tissue Culture Type)
128 were maintained using medium purchased from Gibco (modified eagle's medium (MEM) Gibco
129 (#11095); 10% fetal bovine serum (HI FBS) Gibco (#14000); Penicillin/Streptomycin (PS) Gibco

130 (#15140); 10U/mL penicillin and 10µg/mL streptomycin (only in assay media)). For the SARS-
131 CoV-2 infection induced cytopathic effect (CPE) assay, cells were grown in MEM/10% HI FBS
132 and harvested in MEM/1% PS/supplemented with 2% HI FBS. Cells were batch inoculated with
133 SARS-CoV-2 USA_WA1/2020 (M.O.I. ~ 0.002) which resulted in 5-10% cell viability 72 hours
134 post infection.

135 **Compounds and Preparation of Stock Solutions**

136 The small molecule inhibitors, 5-chloro-7-iodo-8-quinolinol (Clioquinol, CLQ; C0187-Lot JJ01
137 SPGN), and 7-bromo-5-chloro-8-hydroxyquinoline (CLBQ14; B1190-P61JD-FD)); were
138 purchased from TCI America. 5, 7-dichloro-8-hydroxyquinoline (CLCQ; D64600-Lot#STBH7389)
139 and Zinc Chloride (ZnCl₂; 208086-Lot#MKCL1763) were purchased from Sigma Aldrich. We
140 prepared 10mM stocks solutions of the inhibitors in Dimethyl sulfoxide (DMSO; D8418-
141 Lot#SHBL5613) purchased from Sigma Aldrich. For the CPE assay, compound samples were
142 serially diluted 2-fold in DMSO nine times and screened in duplicates. Assay Ready
143 Plates (ARPs; Corning 3764BC) pre-drugged with test compounds (90 nL sample in 100%
144 DMSO per well dispensed using a Labcyte (ECHO 550) are prepared in the Biosafety Level-2
145 (BSL-2) laboratory by adding 5µL assay media to each well.

146 **Method for measuring antiviral effect of CLQ, CLBQ14 and CLCQ:** The SARS-CoV-2
147 infection induced cytopathic effect (CPE) assay and cytotoxicity assays were generated and
148 performed through a sub-contract to Southern Research Institute (SRI), Birmingham, Alabama
149 from Texas Southern University, Houston, Texas. The CPE reduction assay was conducted at
150 SRI to screen for antiviral agents in high throughput screening (HTS) format as previously
151 described^{59,60}. Briefly, Vero E6 cells selected for expression of the SARS-CoV-2 receptor
152 (ACE2; angiotensin-converting enzyme 2) are used for the CPE assay. Cells were grown in
153 MEM/10% HI FBS supplemented and harvested in MEM/1% PS/ supplemented with 2% HI
154 FBS. Cells were batch inoculated with SARS-CoV-2 (M.O.I. ~ 0.002) which resulted in 5% cell
155 viability 72 hours post infection. Compound samples were serially diluted 2-fold in DMSO nine

156 times and screened in duplicates. Assay Ready Plates (ARPs; Corning 3764 BC black-walled,
157 clear bottom plates) pre-drugged with test compounds (90 nL sample in 100% DMSO per well
158 dispensed using a Labcyte (ECHO 550) were prepared in the BSL-2 lab by adding 5µL assay
159 media to each well. The plates were passed into the BSL-3 facility where a 25µL aliquot of virus
160 inoculated cells (4000 Vero E6 cells/well) was added to each well in columns 3-22. The wells
161 in columns 23-24 contained virus infected cells only (no compound treatment). Prior to virus
162 infection, a 25µL aliquot of cells was added to columns 1-2 of each plate for the cell only (no
163 virus) controls. After incubating plates at 37°C/5%CO₂ and 90% humidity for 72 hours, 30µL of
164 Cell Titer-Glo (Promega) was added to each well. Luminescence was read using a Perkin Elmer
165 Envision or BMG CLARIOstar plate reader following incubation at room temperature for 10
166 minutes to measure cell viability. Raw data from each test well was normalized to the average
167 (Avg) signal of non-infected cells (Avg Cells; 100% inhibition) and virus infected cells only (Avg
168 Virus; 0% inhibition) to calculate % inhibition of CPE using the following formula: % inhibition =
169 $100 * (\text{Test Cmpd} - \text{Avg Virus}) / (\text{Avg Cells} - \text{Avg Virus})$. The SARS CPE assay was conducted in
170 BSL-3 containment with plates being sealed with a clear cover and surface decontaminated
171 prior to luminescence reading. Reference compounds for CPE assay were made available by
172 SRI.

173

174 **Method for measuring cytotoxic effect of CLQ, CLBQ14 and CLCQ:** Compound cytotoxicity
175 was assessed in a BSL-2 counter screen as follows using the Cell Titer-Glo Luminescent Cell
176 Viability Assay⁶⁰. Host cells in media were added in 25µL aliquots (4000 cells/well) to each well
177 of assay ready plates prepared with test compounds as above. Cells only (100% viability) and
178 cells treated with hyamine at 100µM final concentration (0% viability) serve as the high and low
179 signal controls, respectively, for cytotoxic effect in the assay. DMSO was maintained at a
180 constant concentration for all wells (0.3%) as dictated by the dilution factor of stock test
181 compound concentrations. After incubating plates at 37°C/5%CO₂ and 90% humidity for 72

182 hours, 30 μ l CellTiter Glo (CTG) (G7573, Promega) was added to each well. Luminescence was
183 read using a BMG CLARIOstar plate reader following incubation at room temperature for 10
184 minutes to measure cell viability.

185 **Biochemical Screening Assays**

186 **ACE2 Inhibitor Screening Assay**

187 An ACE2 Inhibitor screening assay kit with fluorogenic substrate (Catalogue #79923) was
188 purchased from BPS Bioscience (San Diego, CA), and adapted to measure the exopeptidase
189 activity of ACE2 in the presence and absence of inhibitors. The Fluorescence assay was
190 performed using a black flat-bottom 96-well plate with a final reaction volume of 50 μ L following
191 the manufacturer's instructions. We prepared 10mM stock solutions of the compounds in
192 Dimethyl sulfoxide (DMSO). Next, we serially diluted the compounds in DMSO as follows: 100,
193 50, 10, 1, 0.5, and 0.1 μ M for CLQ and CLBQ14; as well as 10 μ M, and 1 μ M for CLCQ. All
194 experiments were performed in triplicates. Each plate contained a positive control of enzyme-
195 treated with vehicle alone (2% DMSO), and a blank control with no enzyme. Briefly, each
196 reaction contained 24 μ L of purified recombinant human ACE2 protein (0.42ng/ μ L) in ACE2
197 buffer, 1 μ L of compound at serially diluted concentrations, and 25 μ L ACE2 fluorogenic
198 substrate. The total reaction volume was 50 μ L. The reaction mixtures were protected from light
199 and incubated for 2.5 hrs at room temperature (22°C). Thereafter, the fluorescence intensities
200 ($\lambda_{\text{Excitation}} = 535\text{nm}$, $\lambda_{\text{Emission}} = 595\text{nm}$) were measured using a Beckman Coulter DTX880
201 multimode plate reader. A similar experiment was conducted to measure and compare the
202 exopeptidase activity of ACE2, in the presence and absence of Zinc Chloride (ZnCl₂) alone,
203 CLBQ14 alone and ZnCl₂ in combination with CLBQ14 at concentrations ranging from 100 μ M to
204 100nM. ZnCl₂ was serially diluted in water, and a positive control of enzyme-treated with vehicle
205 alone (water for ZnCl₂ only; DMSO for CLBQ14 alone; and water plus DMSO for ZnCl₂ and
206 CLBQ14) was carried out for this experiment. The background hydrolysis was subtracted and

207 the data was fitted to a four-parameter logistic (variable slope) equation using GraphPad prism
208 software 8.4.3.

209

210 **The ACE2-Spike (RBD) Protein Interaction assay**

211 A Spike-ACE2 binding assay kit (Cat # CoV-SACE2-1, Lot# 062320 7066) was purchased from
212 RayBiotech (Norcross, GA). The *in vitro* enzyme-linked immunoabsorbent assay (ELISA), was
213 and adapted and performed in a transparent flat-bottom 96-well plate. We prepared 10mM stock
214 solutions of the compounds in Dimethyl sulfoxide (DMSO), with serially diluted the compounds
215 in DMSO as follows: 100, 50, 10, 5, 1, 0.5, and 0.1 μ M for CLQ, CLBQ14 and CLCQ. All
216 experiments were performed in triplicates. Each plate contained positive controls (1% DMSO)
217 and blank controls with no ACE2. Briefly, 1 μ L of serially diluted compounds were incubated
218 with recombinant SARS-CoV-2 Spike receptor binding domain (RBD) protein, pre-coated on the
219 96 well plates in 49 μ L of 1X assay diluent buffer for 31 mins, at room temperature (22°C) with
220 shaking at 180rpm. Next, we added 50 μ L of ACE2 protein in 1X assay diluent buffer into the 96
221 well plate, and incubated for 2.5 hrs at room temperature (22°C) with shaking at 180rpm.
222 Thereafter, the solution was discarded and the plate was washed consecutively four times with
223 300 μ L 1X wash buffer, followed by the addition of the detection antibody (anti-ACE2 goat
224 antibody). The reaction was allowed to go on for 1 hr at room temperature (22°C) with shaking
225 at 180rpm. Then, the solution was discarded and the wash step was repeated as described
226 above. Next, the HRP-conjugated anti-goat IgG was added to each well, and the reaction plate
227 was further incubated for 1 hr at room temperature (22°C) with shaking at 180rpm. Again, the
228 solution was discarded and the wash step was repeated as described above. Then, 100 μ L of
229 3,3',5,5'-tetramethylbenzidine (TMB) one-step substrate was added to each well, and reaction
230 mixtures were incubated in the dark at room temperature (22°C) with shaking at 180rpm for an
231 additional 30 mins and then stopped by the addition of 50 μ L stop solution. The absorbance was
232 read at 405 nm using a Beckman Coulter DTX880 multimode plate reader. The background

233 hydrolysis was subtracted and the data was fitted to a special bell-shaped dose-response curve
234 equation using GraphPad prism software 8.4.3.

235

236 **RESULTS**

237 **Efficacy of Clioquinol (CLQ) and Analogues against SARS-CoV-2 infection induced**

238 **Cytopathic Effect (CPE) in Vero E6 cells.**

239 In our efforts to identify inhibitors of SARS-CoV-2 infection for potential treatment of COVID-19,
240 we evaluated the *in vitro* antiviral activity of CLQ, and two of its derivatives, CLBQ14 and CLCQ,
241 using a standard luminescent-based high-throughput screening (HTS) platform^{59,60} for SARS-
242 CoV-2 infection induced CPE in African Green Monkey Kidney Vero E6 cells. We found that all
243 three compounds inhibited SARS-CoV-2 infection induced CPE *in vitro* with 50% Inhibitory
244 Concentration (IC₅₀) values in the low micromolar concentration (Figure 1). Amongst all three
245 analogues tested, CLQ displayed the most potent antiviral activity in the CPE assay (Figure 1).
246 Compared to its counterparts, CLBQ14 exhibited the highest maximum inhibition at about
247 102.96% inhibition at 30µM (Table 1). In addition, we compared the antiviral effects of CLBQ14
248 and its analogues with five other known inhibitors of SARS-CoV-2 *in vitro*: Chloroquine,
249 Hydroxychloroquine, Remdesivir, Aloxistatin and Calpain Inhibitor IV. The dose-response curves
250 of the CLQ, CLBQ14, CLCQ and the reference compounds mentioned above were determined at
251 multiplicities of infection (MOI) of about 0.002. We found that the IC₅₀ for CLQ (12.62 µM), and its
252 analogues [(CLBQ14, 14.69 µM) and (CLCQ,16.30 µM)] were slightly lower than the IC₅₀ of
253 Aloxistatin (16.72µM); but moderately higher than Chloroquine (1.10µM), Hydroxychloroquine
254 (5.04µM), Remdesivir (4.42µM), and Calpain Inhibitor IV (0.41µM) (Table 2). These results
255 suggest a potential new mechanism of action for CLQ and its congeners. Notably, this is the first
256 report to our knowledge, revealing that CLQ and its analogues effectively inhibit the novel SARS-
257 CoV-2 infection induced CPE.

258

259 **Cytotoxicity Effects of CLQ and Analogues in Vero E6 cells.**

260 We determined the preliminary cytotoxicity of CLQ and its analogues (CLBQ14 and CLCQ),
261 using a Cell Titer-Glo Luminescent Cell Viability Assay⁶⁰. We assessed the cytotoxic effects of
262 the various compounds in Vero E6 cells and observed that, the 50% cytotoxic concentration
263 (CC₅₀) of CLQ and its derivatives were all greater than 30 µM. However, in comparison to the
264 other reference compounds tested, CLQ and its analogues displayed lower percent minimum
265 viability at higher concentrations. On the other hand, we observed similar percent maximum
266 viability for CLQ pharmacophore and the other reference compounds at lower concentrations
267 (Table 3). This suggests that, the cytotoxic effects may not be a concern at lower concentrations
268 of CLQ and its analogues. Additional concentrations need to be tested in future studies to
269 determine the actual CC₅₀ value (Table 3).

270

271 **Effects of CLQ and its Analogues on rhACE2 Exopeptidase Activity**

272 We determined the effect of CLQ, CLBQ14 and CLCQ on the exopeptidase activity of rhACE2
273 using an adapted fluorometric assay (<https://bpsbioscience.com/pub/media/wysiwyg/79923.pdf>).

274 We found that all three compounds inhibited rhACE2 activity with similar IC₅₀ values in the low
275 micromolar concentration, with CLQ being the most potent amongst all three analogues tested,
276 at IC₅₀ of 5.36µM (Table 4). To our knowledge, these results revealed for the first time that,
277 rhACE2 is a biochemical target of CLQ and its analogues. Because, the known metal cofactor
278 for ACE2 is Zinc^{48, 61}, using the same fluorometric assay described above in the methods
279 section, we further assessed the exopeptidase activity of rhACE2, in the presence of Zinc
280 Chloride (ZnCl₂) alone, CLBQ14 alone and ZnCl₂ in combination with CLBQ14 at concentrations
281 ranging from 100µM to 100nM. In the presence of ZnCl₂ alone, rhACE2 displayed increasing
282 exopeptidase activity. On the other hand, in the presence of ZnCl₂ in combination with CLBQ14,
283 we observed an increased shift in IC₅₀ value by over 28 fold compared to CLBQ14 alone (Figure
284 3). Interestingly, this data reveals that increasing concentrations of ZnCl₂, titrates the inhibitory

285 effect of CLBQ14 on rhACE2 from concentrations ranging from above 5 - 10 μ M, consistent with
286 previous reports of the required optimal concentration range of Zinc for the exopeptidase activity
287 of ACE2⁶¹. Taken together, these preliminary results reveal a new pharmacologic mode of
288 action and novel target for CLQ and its analogues.

289

290 **Effects of CLQ and its Analogues on rhACE2 and Spike (RBD) Protein Interaction**

291 The interaction of human ACE2 receptor with SARS-CoV-2's Spike protein receptor binding
292 domain is a critical first step in the process required for viral entry into host cells⁴⁰⁻⁴³. Using an
293 adapted *in vitro* enzyme-linked immunoabsorbent assay (ELISA)
294 (https://doc.raybiotech.com/pdf/Manual/CoV-SACE2_2020.07.09.pdf), we evaluated the effect
295 of CLQ, CLBQ14 and CLCQ on the binding affinity of rhACE2 and RBD of S protein at
296 concentrations ranging from 100 μ M to 100 nM. Surprisingly, we observed a unique bell shaped
297 dose-response curve for all three compounds with higher inhibition of ACE2-Spike (RBD)
298 protein interaction at lower compound concentrations compared to higher concentrations
299 (Figure 4). The bell shaped curve generated two IC₅₀ values (IC_{50_1} and IC_{50_2}) as shown in
300 Table 4. We found that all three compounds had similar IC₅₀ values in the low micromolar
301 concentration ranging from 0.85 μ M to 2.76 μ M for IC_{50_1}; however CLQ displayed a higher
302 IC_{50_2} at 18.15 μ M (Table 4). The unconventional dose response curve observed in this
303 interaction assay, could be an indicator of additional binding site(s) and/or target(s), for the CLQ
304 pharmacophore, such as other sites on ACE2 or the Spike (RBD) protein. Again, these findings
305 are the first report to reveal that CLQ and its analogues inhibit and interfere with the binding
306 between human ACE2 receptor and SARS-CoV-2 Spike RBD protein *in vitro*. These results
307 suggest that the CLQ and its derivatives might be promising leads for clinical development of
308 novel SARS-CoV-2 entry inhibitors and potential COVID-19 therapeutics.

309

310

311 **DISCUSSION**

312 Given the ongoing COVID-19 pandemic and the emerging virulence of novel SARS-
313 CoV-2 strains, there is an urgent need to accelerate the development of effective therapeutic
314 agents as countermeasures against this pathogen. In this study, we applied three independent
315 approaches, to investigate the possibility of CLQ and its analogues as potential inhibitors of the
316 SARS-CoV-2 infection *in vitro*, and gathered strong evidence that this pharmacophore are
317 promising leads for the discovery and pre-clinical development of novel SARS-CoV-2 entry
318 inhibitors and potential COVID-19 therapeutics. To our knowledge, this is the first report
319 revealing rhACE2 as a novel target for CLQ and its analogues, a new pharmacologic mode of
320 action for an old antimicrobial. Taken together, our *in vitro* findings that CLQ significantly
321 inhibited binding of rhACE2 receptor with SARS-CoV-2 Spike (RBD) protein and SARS-CoV-2
322 infection induced CPE, strongly supports the notion that CLQ and its congeners could be
323 potential drugs and/or chemical probes in the development of counter measures against viral
324 entry into host cells.

325 The availability of simple, rapid, cellular high throughput screening and well-characterized
326 biochemical assays enabled us to quickly discover novel inhibitors of SARS-CoV-2 infection *in*
327 *vitro*. We successfully identified and characterized CLQ, a known metal chelator and zinc
328 ionophore, as a novel inhibitor of SARS-CoV-2 infection induced CPE. Using two structural
329 analogues of CLQ (CLBQ14 and CLCQ) in hand, we were able to further explore the impact of the
330 active CLQ pharmacophore on the novel coronavirus infection, the exopeptidase activity of
331 rhACE2 and the interaction of rhACE2 with SARS-CoV-2 Spike (RBD) protein, all critical
332 steps/processes in the pathogenesis of COVID19. All three analogues displayed similar potent
333 inhibition in the low micromolar range, against SARS-CoV-2 infection induced CPE, rhACE2
334 activity and its interaction with Spike Protein. In this study, we also compared the dose-response
335 curves of antiviral effects of CLQ and its analogues with five other known inhibitors of SARS-CoV-
336 2 *in vitro*: Chloroquine, Hydroxychloroquine, Remdesivir, Aloxistatin and Calpain Inhibitor IV and

337 found that CLQ's potency was better and comparable to Aloxistatin; but had lower efficacy than
338 the other reference inhibitors (Table 2). It is important to note that the Vero E6 cells used for the
339 SARS-CoV-2 infection induced CPE assay were first sorted by flow cytometry by SRI for selection
340 of cells that had higher levels of ACE2 expression to increase the efficiency of infection.
341 Therefore, the observed IC₅₀ values may be higher than the actual IC₅₀ values in cells that do not
342 have high levels of ACE2 expression. Moreover, we observed that the IC₅₀ values of the
343 compounds in the biochemical assays were much lower than the IC₅₀ in the cellular antiviral
344 assay. We also assessed the cytotoxic effects of the compounds in Vero E6 cells and observed
345 that CLQ and its analogues displayed lower percent minimum viability at higher concentrations
346 compared to the other reference compounds tested. However, we observed similar percent
347 maximum viability for CLQ pharmacophore and the other reference compounds at lower
348 concentrations (Table 3). This suggests that, the cytotoxic effects may not be a concern at lower
349 concentrations of CLQ and its analogues. In addition, the observed IC₅₀ values for inhibition of
350 rhACE2 exopeptidase activity and rhACE2-RBD interaction were in the low micromolar range,
351 suggesting that we may need lower concentrations for *in vivo* activity. Furthermore, we have other
352 preliminary cytotoxicity results from prior *in vivo* studies on CLQ and its analogues that reveal no
353 significant toxicity at much lower concentrations below nanomolar range (unpublished data).
354 Therefore, additional *in vivo* cytotoxicity studies for Vero E6 cells should be conducted at a wider
355 range of concentrations.

356 Throughout our study, we consistently observed a correlation between the high potency of
357 CLQ compared to its other two analogues in the antiviral screen, inhibition of rhACE2
358 metalloprotease activity, and its ability to disrupt the binding of rhACE2 with SARS-CoV-2 Spike
359 (RBD) protein. Amongst all three compounds, CLQ displayed the highest potency in all three
360 independent assays; except for IC_{50_2}. Hence, validating its potential as a therapeutic option for
361 the treatment of COVID19. Clioquinol and its derivatives belonging to 8-hydroxyquinoline
362 structural class, have been investigated extensively in basic, translational and clinical studies

363 because of their multiple activities as metal chelators and zinc ionophores, modulating underlying
364 molecular and physiologic switches required for metal homeostasis *in vivo*^{14-32, 36-39}. Previously,
365 CLQ was used to treat bacterial infections⁶²; however, it was withdrawn from the clinic because of
366 untoward effects of subacute myelo-optic neuropathy (SMON) mostly experienced in Japan in the
367 1950's^{29,62,63}. More recent studies revealed that SMON might be due to other biologic factors
368 and/or pharmacogenetics primarily linked to the Japanese population^{29, 62,64}. Currently in the clinic,
369 CLQ is approved for use in combination with other agents for treatment of inflammatory skin
370 disorders and fungal infections in some countries^{14,65}. More recently, CLQ and its newer structural
371 derivatives have gained renewed interest as potential drugs for the development of therapeutics
372 for neurodegenerative diseases, cancer, and infectious diseases^{14-32, 36-39}. Furthermore in
373 previous studies, Olaleye O. et. al., serendipitously discovered CLBQ14, the bromine analogue of
374 CLQ and characterized CLQ and additional derivatives as potent inhibitors of replicating and non-
375 replicating *Mycobacterium tuberculosis*, using a HTS assay designed to identify novel
376 metalloprotease inhibitors¹⁷. Altogether, the plethora of evidence on the broad pharmacologic
377 spectrum of activity and metal-chelation propensity of CLQ pharmacophore, combined with its
378 extensive clinical investigational profile, makes this structural class an attractive and promising
379 drugs for targeting ACE2, the important zinc metalloenzyme and essential cellular receptor for
380 SARS-CoV-2 entry into host cells⁴⁰⁻⁴³.

381 ACE2, a carboxypeptidase, is a known type I integral membrane protein made up of about
382 805 amino acids belonging to the large family of Zinc metalloproteases with high level of structural
383 homology for a catalytic motif, containing one characteristic HEXXH + E zinc-binding consensus
384 sequence and binding sites for inhibitor or specific substrates respectively⁴⁸. According to earlier
385 reports by Towler et. al., the first crystalline structures of the metallopeptidase domain of ACE2,
386 revealed "a large inhibitor-dependent hinge bending movement of one catalytic subdomain
387 relative to the other that brings important amino acid residues into position for catalysis," similar to
388 observed subdomains on other zinc metalloproteases respectively⁴⁸. The residues critical for

389 coordinating the binding of Zinc to ACE2 are His³⁷⁴, His³⁷⁸ and Glu⁴⁰², according to earlier x-ray
390 structures⁴⁸. Moreover, ACE2 is activated by monovalent anions and also known to contain an
391 inhibitor-specific anion binding site^{48,61}. The reported optimal metalloprotease activity of
392 recombinant soluble human ACE2 was found to be in the presence of 10 μ M ZnCl₂⁶¹. This is
393 consistent with our findings of rhACE2 exopeptidase activity assay, in the presence of Zinc
394 Chloride (ZnCl₂). In the presence of the newly identified potent metalloprotease inhibitors (CLQ or
395 CLBQ14 alone), we observed a significantly decreased exopeptidase activity for ACE2 in the low
396 micromolar concentrations (Figure 4). However, we found an increased shift in IC₅₀ values when
397 we assessed exopeptidase activity in the presence of ZnCl₂ in combination with CLBQ14 by over
398 28 fold compared to CLBQ14 alone (Figure 3), suggesting that CLBQ14, might be working
399 through zinc chelation, interaction and/or coordination. Our findings not only revealed a novel
400 target (rhACE2) and mechanism of action for the CLQ pharmacophore; but also provides insight
401 into potential reversibility of inhibition and one or more probable mode(s) of inhibition: 1) The
402 concentration of CLBQ14 is titrated with excess ZnCl₂, thus pre-occupied and unavailable to
403 inhibit rhACE2 exopeptidase activity; and/or 2) potential competition for the similar binding sites
404 on rhACE2. Additional mechanistic kinetic studies will be required to ascertain this notion.

405 Moreover as mentioned earlier, ACE2, plays an essential role in the regulation of
406 cardiovascular and respiratory physiology^{47,48}. Its characterization as the functional host receptor
407 for entry of the novel SARS-CoV-2 into human cells⁴⁰⁻⁴³, has raised concerns about the potential
408 impact of newly discovered ACE2 inhibitors on cardiovascular and respiratory physiology⁶⁶⁻⁶⁸.
409 Recent studies have also shown that ACE2 plays a key role in protecting the lungs from
410 ARDS^{67,68}, a severe complication of COVID-19 disease⁴. Therefore, one has to proceed
411 cautiously when targeting ACE2⁶⁶; without permanently inactivating its exopeptidase or other
412 cellular functions, to avoid potential adverse effects to heart and/or lung function. Our lead
413 compound CLQ is a weak metal chelator and zinc ionophore, that can shuttle free zinc across the
414 membrane^{31,69}. Because of these properties, CLQ may temporarily or reversibly affect ACE2

415 function and prevent its interaction with SARS-CoV-2 RBD protein; without permanently inhibiting
416 its essential exopeptidase function. Because rhACE2 is a novel host target for CLQ and its
417 analogues, the potential effect of CLQ inhibition on heart and lung function needs to be further
418 explored *in vivo* and pre-clinical studies.

419 The crystal structure of full length human ACE2 revealed that the RBD on SARS-CoV-2
420 S1 binds directly to the metallopeptidase domain (MPD) of ACE2 receptor^{40,41}, that consists of
421 amino acid residues that coordinates zinc, providing further support for the utility of zinc chelators
422 and/or ionophores such as CLQ and its congeners, as promising inhibitors of interaction and viral
423 entry inhibitors. Using a sensitive ELISA, we found that CLQ and its analogues potently disrupt
424 the interaction of ACE2 and Spike (RBD) protein, with CLQ being the most potent. Thus,
425 supporting our findings showing that CLQ and its derivatives binds to ACE2 and inhibits
426 exopeptidase activity. Interestingly unlike the CLQ pharmacopore, other studies revealed that
427 (S,S)-2-{1-Carboxy-2-[3-(3,5-dichloro-benzyl)-3H-imidazol-4-yl]-ethylamino}-4-methyl-pentanoic
428 acid (MLN-4760), a known potent inhibitor of ACE2 exopeptidase activity, belonging to a different
429 chemical class, does not disrupt ACE2-Spike interaction in coronaviruses, SARS-CoV, SARS-
430 CoV2, and NL63S^{70,71} as its binding site on ACE2 is different than the site where RBD interacts
431 with ACE2^{48,70,72}. However, CLQ seems to affect ACE2 by reversibly chelating its zinc ion which
432 is essential for ACE2 activity, as well as interfere with ACE2-RBD interaction. Although zinc is
433 essential for stabilizing protein structures and altering the substrate affinity of different
434 metalloproteins^{32,73}, the effects of zinc chelation on molecular structure of ACE2 and its effects on
435 its binding to the SARS-CoV-2 remains to be tested. Moreover, earlier molecular and structural
436 studies also revealed that mutations in the catalytic site required for exopeptidase activity of
437 ACE2, had no effect on Spike RBD binding to ACE2⁴⁸. Howbeit, the unconventional dose-
438 response bell shaped curve that we observed in our studies suggests that there may be additional
439 binding sites and/or modes of action for CLQ and its congeners, resulting in the potent inhibition
440 of interaction at lower micromolar concentrations; compared to higher concentrations. Although,

441 CLQ was found to be the most potent amongst all 3 analogs, except for IC_{50_2}, preliminary SAR
442 revealed that the other two derivatives are comparable to CLQ, as they both show potent
443 inhibition of rhACE2-RBD interaction, as well as inhibition of antiviral and anti-rhACE2 activity.
444 Therefore, providing alternative analogues that might not have the same adverse effects
445 experienced with CLQ in the past, potentially alleviating some of the concerns with CLQ.
446 Additional biochemical and structural studies are required to explore other possible mechanisms
447 of action such as competition or interaction of CLQ with RBD for binding to MPD of ACE2, thereby
448 preventing zinc chelation and ionophore activity of CLQ. Future X-ray structures could help to
449 better understand mode of inhibition of this pharmacophore and rational design of more potent
450 drugs.

451 The strengths of our study includes, the use of a rapid multi-prong approach via three
452 sensitive independent assays, to identify and characterize an existing clinical drug as a novel
453 inhibitor of SARS-CoV-2 infection *in vitro*. In addition, the availability of structural analogues of
454 CLQ, made possible a preliminary structure activity relationship studies (SAR), which revealed
455 similarity between the IC₅₀ values of CLQ and its structural analogues. However, our study has
456 some limitations such as the use of Vero E6 cells that were selected for high expression of
457 ACE2 in the antiviral assay, a HTS designed to rapidly screen for inhibitors of infection induced
458 CPE. An additional limitation is that, the amount of zinc in the purified rhACE2 supplied from
459 BPS and RayBiotech assays were unknown. Future metal dependent studies with apoenzymes
460 will be required to determine the amount of zinc. Considering that CLQ is a known zinc chelator
461 and ionophore, an understanding of the physiologic amount of zinc required for inhibition will be
462 critical for optimal efficacy. Therefore, for these two limitations, the measured IC₅₀ values for the
463 compounds may not be representative of the actual *in vitro* IC₅₀, which may be lower. However,
464 the remarkable consistency in the observed strong correlation between CLQ and its congener's
465 antiviral activity, *in vitro* rhACE2 inhibition and disruption of ACE2-RBD protein interaction,
466 reduces these concerns.

467

468 **CONCLUSION AND SIGNIFICANCE**

469 The impact of the COVID-19 pandemic on human health, healthcare systems, and the global
470 economy⁷⁴ has imposed an urgent call/pressing need for the development of novel antivirals.
471 Rapid clinical development of anti-COVID19 treatments could be accelerated by discovery of re-
472 purposed clinically approved drugs with new mechanisms of action and/or multiple cellular
473 targets that could potentially disrupt viral pathogenesis/survival and/or prevent the viral
474 entry/interaction with host receptor, ACE2. The body of evidence on the broad pharmacologic
475 spectrum of activity, metal-chelation propensity and zinc ionophore activity of CLQ
476 pharmacophore, combined with its extensive clinical investigational profile, makes this structural
477 class, attractive and promising drugs for targeting rhACE2. Using a multi-prong approach, we
478 discovered and characterized CLQ, a clinical drug and two of its analogues (CLBQ14 and
479 CLCQ) as potent inhibitors of SARS-CoV-2 infection induced CPE *in vitro*; rhACE2
480 metalloprotease activity; and the binding of rhACE2 with SARS-CoV-2 Spike (RBD) protein.
481 Altogether, these novel findings provide insights into a new mode of action and molecular
482 target(s) for CLQ and its derivatives. Thus, validating this structural class as promising leads for
483 clinical development of novel SARS-CoV-2 entry inhibitors and potential COVID-19
484 therapeutics. Because rhACE2 is a host target, it reduces the concerns for development of drug
485 resistance, which is usually seen with drugs that target viral genes. Further SAR,
486 computational/molecular modeling and X-crystal structure studies will aid the rational design
487 and synthesis of more potent inhibitors in the CLQ-containing, 8-hydroxyquinoline structural
488 class. Our studies not only provides an additional new drug class with zinc chelating and
489 ionophore properties, in the pipeline for urgent quest for therapeutic management for anti-
490 COVID19, but also suggests that there could be the potential physiologic relevance of zinc
491 homeostatis in SARS-CoV-2 infection and COVID19 pathogenesis. In addition, CLQ and its
492 derivatives could be used as chemical probes to study the biology of host-pathogen interaction

493 in the context of SARS-CoV-2 infections. In the future, the functional importance of molecular
494 and cellular regulation of host and viral zinc dependent genes/proteins in SARS-CoV-2
495 pathogenesis and survival may be better understood and targeted with available zinc chelators,
496 ionophores, and transporters. Moreover, unlike MLN-4670 another known ACE2 inhibitor^{48,70,71},
497 our results not only show that CLQ and its analogues inhibits rhACE2, with antiviral activity, but
498 also suggests that CLQ pharmacophore, potentially disrupts the interaction of rhACE2 and Spike
499 (RBD) protein. To this end, we provide strong cellular and biochemical evidence supporting the
500 notion that CLQ, CLBQ14 and CLCQ, could serve as a potential lead series for the pre-clinical
501 development of new anti-COVID19 treatments. The expectation is that the development of new
502 anti-COVID19 treatments with dual activity against viral and host entry target could help combat
503 the issue of emerging drug resistant strains, drug-drug interactions, reduction in the cost of
504 treatment, possibly increase patient compliance and improve patient care as well as reduce the
505 mortality rate due to SARS-CoV-2 infection. Therefore, we propose pharmacologic and clinical
506 studies to further explore CLQ and/or its derivatives as treatment options in the tool box for
507 combating this novel coronavirus, and be evaluated in conjunction with other available
508 therapeutics to reduce COVID19 morbidity and mortality as well as potential drug to drug
509 interactions⁷⁵⁻⁷⁸ encountered with other drugs.

510

511 **Author Contributions:** OAO conceived the study and performed biochemical experiments
512 (rhACE2 inhibitor screening assay and rhACE2-Spike (RBD) protein interaction experiments);
513 OAO and MK performed experimental design, data analysis and interpretations. OAO, MK, CO
514 and TA wrote the manuscript.

515

516 **Funding:** This work was supported in part by research infrastructure support from grant number
517 5G12MD007605-26 from the NIMHD/NIH.

518 **Competing interest:** The authors declare no competing interests.

519 **References**

- 520 1. World Health Organization (WHO) Director-General's opening remarks at the media briefing on
521 COVID-19, (2020).
- 522 2. WHO Coronavirus disease 2019 (COVID-19) Situation Report – 46– 6 March, (2020).
- 523 3. Zhu, N. *et al.* A novel coronavirus from patients with pneumonia in China, 2019. *New England*
524 *Journal of Medicine* **382**, (2020).
- 525 4. Huang, C. *et al.* Clinical features of patients infected with 2019 novel coronavirus in Wuhan,
526 China. *The Lancet* **395**, (2020).
- 527 5. Madjid, M., Safavi-Naeini, P., Solomon, S. D. & Vardeny, O. Potential Effects of Coronaviruses
528 on the Cardiovascular System: A Review. *JAMA Cardiology* (2020).
529 doi:10.1001/jamacardio.2020.1286.
- 530 6. Mao, L. *et al.* Neurological Manifestations of Hospitalized Patients with COVID-19 in Wuhan,
531 China: A Retrospective Case Series Study. *SSRN Electronic Journal* (2020)
532 doi:10.2139/ssrn.3544840.
- 533 7. Guan, W. *et al.* Clinical characteristics of coronavirus disease 2019 in China. *New England*
534 *Journal of Medicine* **382**, (2020).
- 535 8. Potential Antiviral Drugs Under Evaluation for the Treatment of COVID-19, *National institute of*
536 *Health (NIH), COVID-19 Treatment Guidelines, July 24 (2020)*. Retrieved from
537 <https://www.covid19treatmentguidelines.nih.gov/antiviral-therapy/>
- 538 9. Sanders, J. M., Monogue, M. L., Jodlowski, T. Z. & Cutrell, J. B. Pharmacologic Treatments for
539 Coronavirus Disease 2019 (COVID-19): A Review. *JAMA - Journal of the American Medical*
540 *Association* vol. 323 (2020).
- 541 10. Slomski, A. No Benefit for Lopinavir–Ritonavir in Severe COVID-19. *JAMA* 323, 1999 (2020).
- 542 11. Horby, P. *et al.* Effect of Dexamethasone in Hospitalized Patients with COVID-19: Preliminary
543 Report. (2020). doi:10.1101/2020.06.22.20137273

- 544 12. Verma, H. et al. Current updates on the European and WHO registered clinical trials of
545 coronavirus disease 2019 (COVID-19). *Biomedical Journal* (2020).doi:10.1016/j.bj.2020.07.008
- 546 13. Coronavirus (COVID-19) Update: FDA Issues Emergency Use Authorization for Potential
547 COVID-19 Treatment, May 1 (2020). Retrieved from [https://www.fda.gov/news-events/press-](https://www.fda.gov/news-events/press-announcements/coronavirus-covid-19-update-fda-issues-emergency-use-authorization-potential-covid-19-treatment)
548 [announcements/coronavirus-covid-19-update-fda-issues-emergency-use-authorization-](https://www.fda.gov/news-events/press-announcements/coronavirus-covid-19-update-fda-issues-emergency-use-authorization-potential-covid-19-treatment)
549 [potential-covid-19-treatment](https://www.fda.gov/news-events/press-announcements/coronavirus-covid-19-update-fda-issues-emergency-use-authorization-potential-covid-19-treatment)
- 550 14. You, Z., Ran, X., Dai, Y. & Ran, Y. Clioquinol, an alternative antimicrobial agent against
551 common pathogenic microbe. *Journal de Mycologie Medicale* **28**, (2018).
- 552 15. Bednarz-Prashad, A. J. & John, E. I. Effect of clioquinol, an 8-hydroxyquinoline derivative, on
553 rotavirus infection in mice. *The Journal of infectious diseases* **148**, (1983).
- 554 16. Auld, D. S., Kawaguchi, H., Livingston, D. M. & Vallee, B. L. RNA dependent DNA polymerase
555 (reverse transcriptase) from avian myeloblastosis virus: a zinc metalloenzyme. *Proceedings of*
556 *the National Academy of Sciences of the United States of America* **71**, 2091–2095 (1974).
- 557 17. Olaleye, O. et al. Characterization of Clioquinol and Analogs as Novel Inhibitors of Methionine
558 Aminopeptidases from *Mycobacterium tuberculosis*. *Tuberculosis (Edinb)*, [https://doi:](https://doi.org/10.1016/j.tube.2011.10.012)
559 [10.1016/j.tube.2011.10.012](https://doi.org/10.1016/j.tube.2011.10.012) (2011).
- 560 18. Darby, C. M. & Nathan, C. F. Killing of non-replicating *Mycobacterium tuberculosis* by 8-
561 hydroxyquinoline. *Journal of Antimicrobial Chemotherapy* **65**, (2010).
- 562 19. Tavares, G. de S. V. et al. Antileishmanial Activity, Cytotoxicity and Mechanism of Action of
563 Clioquinol Against *Leishmania infantum* and *Leishmania amazonensis* Species. *Basic and*
564 *Clinical Pharmacology and Toxicology* **123**, (2018).
- 565 20. Bohlmann, L. et al. Chemical synergy between ionophore PBT2 and zinc reverses antibiotic
566 resistance. *mBio* **9**, (2018).
- 567 21. Schimmer, A. D. et al. A phase I study of the metal ionophore clioquinol in patients with
568 advanced hematologic malignancies. *Clinical Lymphoma, Myeloma and Leukemia* **12**, (2012).

- 569 22. Ayton, S., Lei, P. & Bush, A. I. Biometals and Their Therapeutic Implications in Alzheimer's
570 Disease. *Neurotherapeutics* vol. 12 (2015).
- 571 23. Tavares, G. S. V. *et al.* A clioquinol-containing Pluronic®F127 polymeric micelle system is
572 effective in the treatment of visceral leishmaniasis in a murine model. *Parasite* **27**, (2020).
- 573 24. Cherny, R. A. *et al.* PBT2 reduces toxicity in a *C. elegans* model of polyQ aggregation and
574 extends lifespan, reduces striatal atrophy and improves motor performance in the R6/2 mouse
575 model of Huntington's disease. *Journal of Huntington's Disease* **1**, (2012).
- 576 25. Lannfelt, L. *et al.* Safety, efficacy, and biomarker findings of PBT2 in targeting Abeta as a
577 modifying therapy for Alzheimer's disease: a phase IIa, double-blind, randomised, placebo-
578 controlled trial. *The Lancet Neurology* vol. 7 (2008).
- 579 26. Ritchie, C. W. *et al.* Metal-Protein Attenuation with Iodochlorhydroxyquin (Clioquinol) Targeting
580 A β Amyloid Deposition and Toxicity in Alzheimer Disease: A Pilot Phase 2 Clinical Trial.
581 *Archives of Neurology* **60**, (2003).
- 582 27. Adlard, P. A. *et al.* Rapid Restoration of Cognition in Alzheimer's Transgenic Mice with 8-
583 Hydroxy Quinoline Analogs Is Associated with Decreased Interstitial A β . *Neuron* **59**, (2008).
- 584 28. Shi, L. *et al.* Clioquinol improves motor and non-motor deficits in MPTP-induced monkey model
585 of Parkinson's disease through AKT/mTOR pathway. *Aging* **12**, (2020).
- 586 29. Perez, D. R., Sklar, L. A. & Chigaev, A. Clioquinol: To harm or heal. *Pharmacology and*
587 *Therapeutics* vol. 199 (2019).
- 588 30. McInerney, M. P. *et al.* Ionophore and Biometal Modulation of P-glycoprotein Expression and
589 Function in Human Brain Microvascular Endothelial Cells. *Pharmaceutical Research* **35**,
590 (2018).
- 591 31. Yu, H., Zhou, Y., Lind, S. E. & Ding, W. Q. Clioquinol targets zinc to lysosomes in human
592 cancer cells. *Biochemical Journal* **417**, (2009).
- 593 32. Ding, W. Q., Lin, B., Vaught, J. L., Yamauchi, H. & Lind, S. E. Anticancer activity of the
594 antibiotic clioquinol. *Cancer Research* (2005) doi:10.1158/0008-5472.CAN-04-3577.

- 595 33. Choi, Y., Bowman, J. W. & Jung, J. U. Autophagy during viral infection - A double-edged
596 sword. *Nature Reviews Microbiology* vol. 16 (2018).
- 597 34. Lowther, W. T. & Matthews, B. W. Structure and function of the methionine aminopeptidases.
598 *Biochimica et Biophysica Acta - Protein Structure and Molecular Enzymology* vol. 1477 (2000).
- 599 35. Giglione, C., Vallon, O. & Meinel, T. Control of protein life-span by N-terminal methionine
600 excision. *EMBO Journal* **22**, (2003).
- 601 36. Haase, H., Overbeck, S. & Rink, L. Zinc supplementation for the treatment or prevention of
602 disease: Current status and future perspectives. *Experimental Gerontology* vol. 43 (2008).
- 603 37. Lind, S. E., Park, J. S. & Drexler, J. W. Pyriithione and 8-hydroxyquinolines transport lead
604 across erythrocyte membranes. *Translational Research* **154**, (2009).
- 605 38. Andersson, D. A., Gentry, C., Moss, S. & Bevan, S. Clioquinol and pyriithione activate TRPA1
606 by increasing intracellular Zn²⁺. *Proceedings of the National Academy of Sciences of the*
607 *United States of America* **106**, (2009).
- 608 39. Ding, W. Q., Yu, H. J. & Lind, S. E. Zinc-binding compounds induce cancer cell death via
609 distinct modes of action. *Cancer Letters* **271**, (2008).
- 610 40. Wrapp, D. *et al.* Cryo-EM structure of the 2019-nCoV spike in the prefusion conformation.
611 *Science* (2020) doi:10.1126/science.aax0902.
- 612 41. Yan, R. *et al.* Structural basis for the recognition of SARS-CoV-2 by full-length human ACE2.
613 *Science* (2020) doi:10.1126/science.abb2762.
- 614 42. Wang, Q. *et al.* Structural and Functional Basis of SARS-CoV-2 Entry by Using Human ACE2.
615 *Cell* **181**, (2020).
- 616 43. Walls, A. C. *et al.* Structure, Function, and Antigenicity of the SARS-CoV-2 Spike Glycoprotein.
617 *Cell* **181**, (2020).
- 618 44. Hamming, I. *et al.* Tissue distribution of ACE2 protein, the functional receptor for SARS
619 coronavirus. A first step in understanding SARS pathogenesis. *Journal of Pathology* (2004)
620 doi:10.1002/path.1570.

- 621 45. Harmer, D., Gilbert, M., Borman, R. & Clark, K. L. Quantitative mRNA expression profiling of
622 ACE 2, a novel homologue of angiotensin converting enzyme. *FEBS Letters* (2002)
623 doi:10.1016/S0014-5793(02)03640-2.
- 624 46. Warner, F. J., Guy, J. L., Lambert, D. W., Hooper, N. M. & Turner, A. J. Angiotensin converting
625 enzyme-2 (ACE2) and its possible roles in hypertension, diabetes and cardiac function. *Letters*
626 *in Peptide Science* (2003) doi:10.1007/BF02442567.
- 627 47. Kuba, K. *et al.* A crucial role of angiotensin converting enzyme 2 (ACE2) in SARS coronavirus-
628 induced lung injury. *Nature Medicine* (2005) doi:10.1038/nm1267.
- 629 48. Towler, P. *et al.* ACE2 X-Ray Structures Reveal a Large Hinge-bending Motion Important for
630 Inhibitor Binding and Catalysis. *Journal of Biological Chemistry* **279**, 17996–18007 (2004).
- 631 49. Li, F., Li, W., Farzan, M. & Harrison, S. C. Structural biology: Structure of SARS coronavirus
632 spike receptor-binding domain complexed with receptor. *Science* **309**, (2005).
- 633 50. Li, F. Receptor Recognition Mechanisms of Coronaviruses: a Decade of Structural Studies.
634 *Journal of Virology* **89**, (2015).
- 635 51. Song, W., Gui, M., Wang, X. & Xiang, Y. Cryo-EM structure of the SARS coronavirus spike
636 glycoprotein in complex with its host cell receptor ACE2. *PLoS Pathogens* (2018)
637 doi:10.1371/journal.ppat.1007236.
- 638 52. Kam, Y. W. *et al.* Cleavage of the SARS coronavirus spike glycoprotein by airway proteases
639 enhances virus entry into human bronchial epithelial cells in vitro. *PLoS ONE* **4**, (2009).
- 640 53. Hoffmann, M. *et al.* SARS-CoV-2 Cell Entry Depends on ACE2 and TMPRSS2 and Is Blocked
641 by a Clinically Proven Protease Inhibitor. *Cell* **181**, (2020).
- 642 54. Belouzard, S., Chu, V. C. & Whittaker, G. R. Activation of the SARS coronavirus spike protein
643 via sequential proteolytic cleavage at two distinct sites. *Proceedings of the National Academy*
644 *of Sciences of the United States of America* (2009) doi:10.1073/pnas.0809524106.
- 645 55. Kirchdoerfer, R. N. *et al.* Pre-fusion structure of a human coronavirus spike protein. *Nature*
646 **531**, (2016).

- 647 56. Gui, M. *et al.* Cryo-electron microscopy structures of the SARS-CoV spike glycoprotein reveal a
648 prerequisite conformational state for receptor binding. *Cell Research* **27**, (2017).
- 649 57. Millet, J. K. & Whittaker, G. R. Host cell proteases: Critical determinants of coronavirus tropism
650 and pathogenesis. *Virus Research* **202**, (2015).
- 651 58. Madu, I. G., Roth, S. L., Belouzard, S. & Whittaker, G. R. Characterization of a Highly
652 Conserved Domain within the Severe Acute Respiratory Syndrome Coronavirus Spike Protein
653 S2 Domain with Characteristics of a Viral Fusion Peptide. *Journal of Virology* **83**, (2009).
- 654 59. Maddox, C. B., Rasmussen, L. & White, E. L. Adapting Cell-Based Assays to the High-
655 Throughput Screening Platform: Problems Encountered and Lessons Learned. *Journal of*
656 *Laboratory Automation* **13**, (2008).
- 657 60. Severson, W. E. *et al.* Development and validation of a high-throughput screen for inhibitors of
658 SARS CoV and its application in screening of a 100,000-compound library. *Journal of*
659 *Biomolecular Screening* **12**, (2007).
- 660 61. Vickers, C. *et al.* Hydrolysis of biological peptides by human angiotensin-converting enzyme-
661 related carboxypeptidase. *Journal of Biological Chemistry* **277**, (2002).
- 662 62. Cahoon, L. The curious case of clioquinol. *Nature Medicine* **15**, (2009).
- 663 63. Kono, R. Subacute myelo-optico-neuropathy, a new neurological disease prevailing in japan.
664 *Japanese Journal of Medical Science and Biology* **24**, (1971).
- 665 64. Meade, T. W. Subacute myelo optic neuropathy and clioquinol. An epidemiological case history
666 for diagnosis. *British Journal of Preventive and Social Medicine* vol. 29 (1975).
- 667 65. Mao, X. & Schimmer, A. D. The Toxicology of Clioquinol. *Toxicology Letters* vol. 182 (2008).
- 668 66. South, A. M., Diz, D. I. & Chappell, M. C. COVID-19, ACE2, and the cardiovascular
669 consequences. *American journal of physiology. Heart and circulatory physiology* **318**, (2020).
- 670 67. Nishiga, M., Wang, D.W., Han, Y., Lewis, D.B., & Wu, J.C. COVID-19 and cardiovascular
671 disease: from basic mechanisms to clinical perspectives. *Nat Rev Cardiol* (2020).

- 672 68. Imai, Y. *et al.* Angiotensin-converting enzyme 2 protects from severe acute lung failure. *Nature*
673 **436**, 112–116 (2005).
- 674 69. Colvin, R. A. *et al.* Insights into Zn²⁺ homeostasis in neurons from experimental and modeling
675 studies. *American Journal of Physiology - Cell Physiology* **294**, (2008).
- 676 70. Nami, B., Ghanaeian, A., Ghanaeian, K. & Nami, N. The Effect of ACE2 Inhibitor MLN-4760 on
677 the Interaction of SARS-CoV-2 Spike Protein with Human ACE2: A Molecular Dynamics Study.
678 (2020) doi:10.26434/chemrxiv.12159945.
- 679 71. Mathewson, A. C. *et al.* Interaction of severe acute respiratory syndrome-coronavirus and
680 NL63 coronavirus spike proteins with angiotensin converting enzyme-2. *Journal of General*
681 *Virology* **89**, (2008).
- 682 72. Li, W. *et al.* Receptor and viral determinants of SARS-coronavirus adaptation to human ACE2.
683 *EMBO Journal* **24**, (2005).
- 684 73. Cox, E. H. & McLendon, G. L. Zinc-dependent protein folding. *Current Opinion in Chemical*
685 *Biology* vol. 4 (2000).
- 686 74. Chaudhry, R., Dranitsaris, G., Mubashir, T., Bartoszko, J. & Riazi, S. A country level analysis
687 measuring the impact of government actions, country preparedness and socioeconomic factors
688 on COVID-19 mortality and related health outcomes. *EClinicalMedicine* **0**, 100464 (2020).
- 689 75. Zhang, M. *et al.* Electrophysiologic Studies on the Risks and Potential Mechanism Underlying
690 the Proarrhythmic Nature of Azithromycin. *Cardiovasc Toxicol*, [https:// DOI: 10.1007/s12012-](https://doi.org/10.1007/s12012-017-9401-7)
691 [017-9401-7](https://doi.org/10.1007/s12012-017-9401-7) (2017).
- 692 76. Capel, R.A. *et al.* Hydroxychloroquine reduces heart rate by modulating the hyperpolarization-
693 activated current I_f: Novel electrophysiological insights and therapeutic potential. *Heart Rhythm*
694 **12**, 2186-2194, [https://doi: 10.1016/j.hrthm.2015.05.027](https://doi.org/10.1016/j.hrthm.2015.05.027) (2015).
- 695 77. Plasencia-Garcia, B.O. *et al.* Drug-Drug interactions between COVID-19 treatments and
696 antipsychotics drugs: integrated evidence from 4 databases and a systematic review.
697 <https://doi.org/10.1101/2020.06.04.20122416>

698 78. Roden, Dan M., et al. "Considerations for drug interactions on QTc in exploratory COVID-19
699 (coronavirus disease 2019) treatment." *Circulation* (2020).

700

701 **Figures and Tables** (See attached)

702 **Figure 1.** Efficacy of Clioquinol (CLQ) and Analogues against SARS-CoV-2 induced Cytopathic
703 Effect (CPE) in Vero E6 cells: A. CLBQ14, B. CLCQ, and C. CLQ.

704

705 **Figure 2.** Efficacy of Reference Inhibitors against SARS-CoV-2 induced Cytopathic Effect
706 (CPE) in Vero E6 cells: A. CalpainInhibitorIV, B. Chloroquine, C Remdesivir, D.
707 Hydroxychloroquine, and E. E64d (Aloxistatin).

708

709 **Figure 3.** Effect of Clioquinol (CLQ) and Analogues against ACE2 Exopeptidase Activity: A.
710 CLBQ14 (Circles - red), B. CLQ (Squares - green), and C. ZnCl₂ (Triangle – blue), and D.
711 CLBQ14 and ZnCl₂ (Inverted Triangles – magenta).

712

713 **Figure 4.** Inhibition of ACE2 and SARS-CoV-2 Spike (RBD) Protein Interaction by Clioquinol
714 (CLQ) and Analogues: A. CLBQ14, B. CLCQ, and C. CLQ.

715

716 **Table 1.** Chemical Structure and Activity of Clioquinol (CLQ) and Analogues against SARS-
717 CoV-2 induced Cytopathic Effect (CPE) in Vero E6 Cells.

718

719 **Table 2.** Chemical Structure and Activity of Reference Inhibitors against SARS-CoV-2 induced
720 Cytopathic Effect (CPE) in Vero E6 Cells.

721

722 **Table 3.** Cytotoxicity of Clioquinol (CLQ) and Analogues in Vero E6 Cells, in Comparison to
723 Reference Inhibitors of SARS-CoV-2.

724

725 **Table 4.** Activity of Clioquinol (CLQ) and Analogues against ACE2 Exopeptidase Activity and
726 ACE2 and SARS-CoV-2 Spike (RBD) Protein Interaction.

727

728

729

730

731

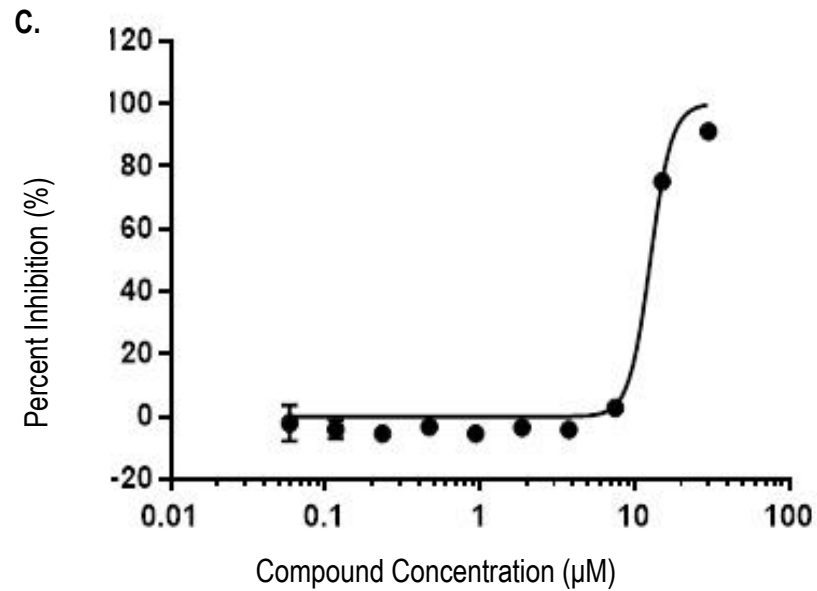
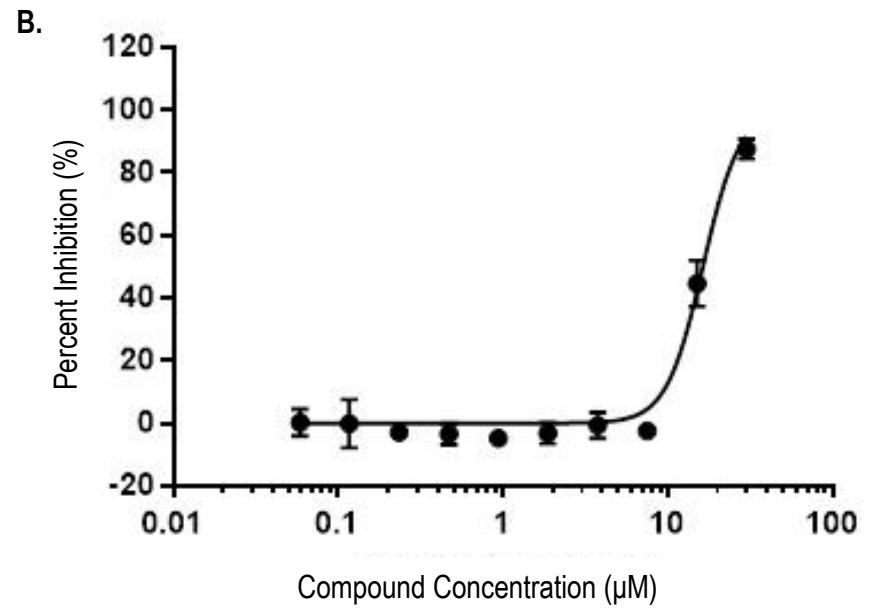
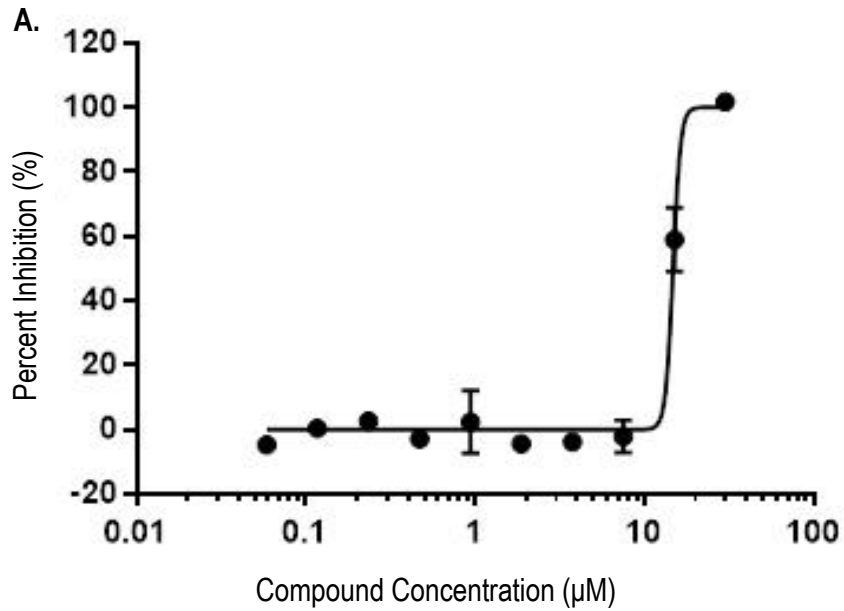


Figure 1. Efficacy of Clioquinol (CLQ) and Analogues against SARS-CoV-2 induced Cytopathic Effect (CPE) in Vero E6 cells : A. CLBQ14, B. CLCQ, and C. CLQ.

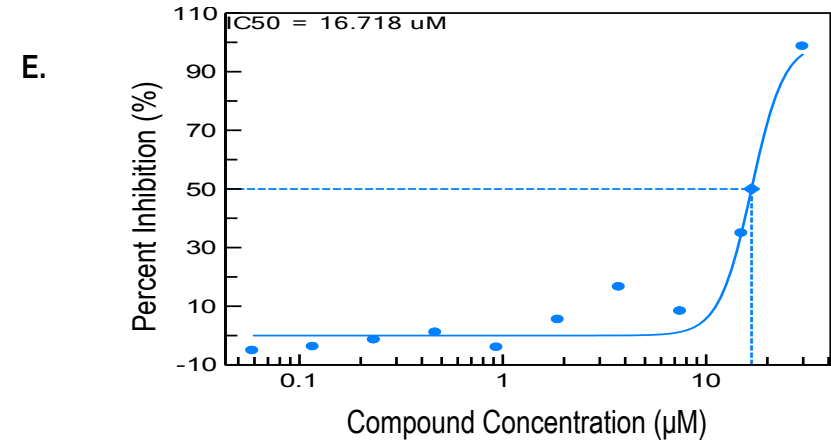
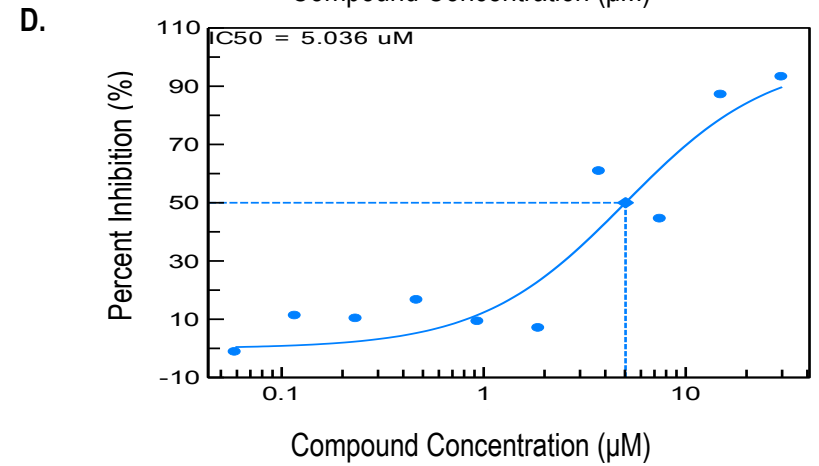
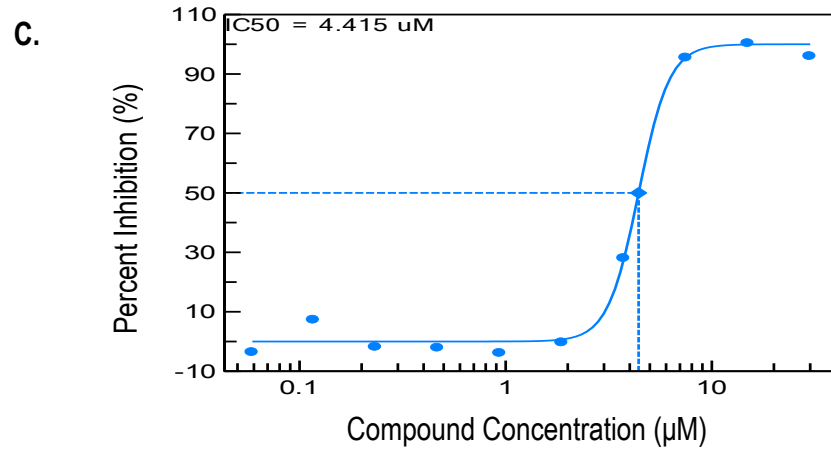
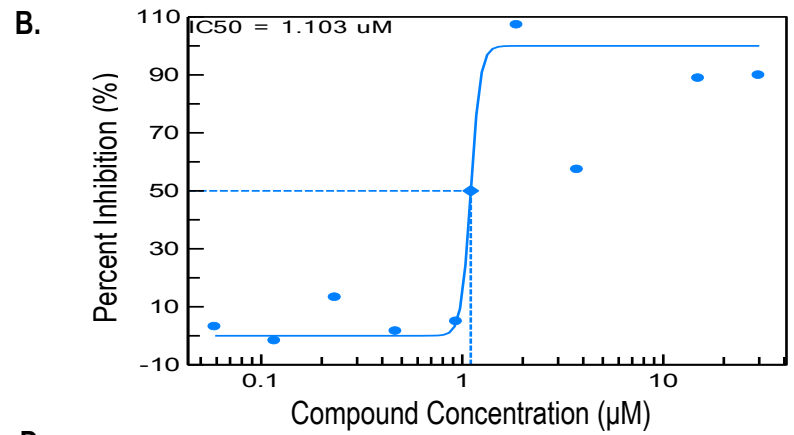
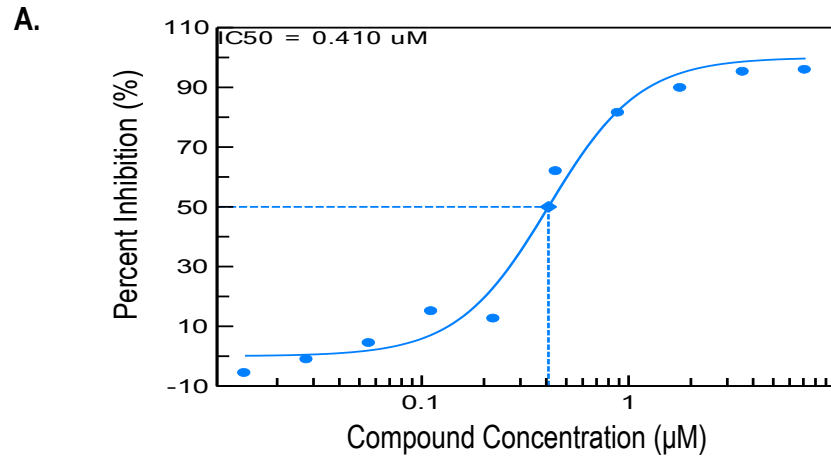


Figure 2. Efficacy of Reference Inhibitors against SARS-CoV-2 induced Cytopathic Effect (CPE) in Vero E6 cells: A. CalpainInhibitorIV, B. Chloroquine, C Remdesivir, D. Hydroxychloroquine and E. E64d (Aloxistatin).

Table 1. Chemical Structure and Activity of Clioquinol (CLQ) and Analogues against SARS-CoV-2 induced Cytopathic Effect (CPE) in Vero E6 Cells.

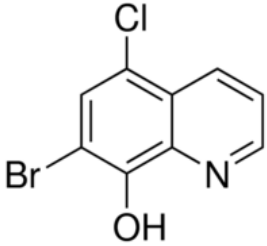
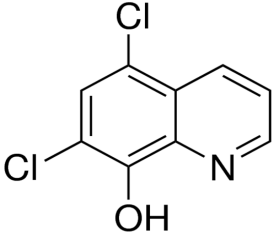
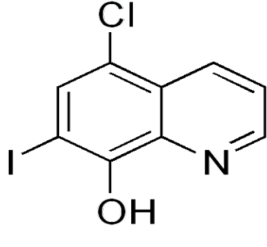
Inhibitor ID	Screen ID	Chemical Structure	IC ₅₀ (μM)	Maximum Inhibition at 30μM (%)
CLBQ14	MDXC19T001		14.69	102.96
CLCQ	MDXC19T002		16.30	89.78
CLQ	MDXC19T003		12.62	91.78

Table 2. Chemical Structure and Activity of Reference Inhibitors against SARS-CoV-2 induced Cytopathic Effect (CPE) in Vero E6 Cells.

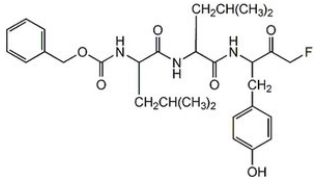
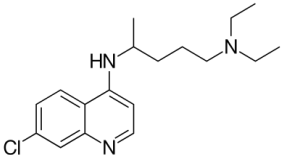
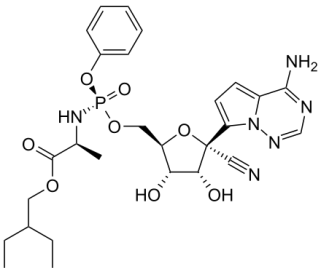
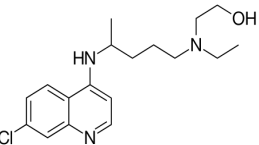
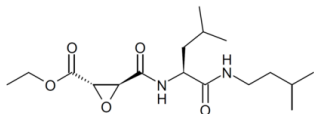
Inhibitor ID	Screen ID	Chemical Structure	IC ₅₀ (μM)	Maximum Inhibition (%)	Concentration at Maximum % Inhibition (μM)
CalpainInhibitorIV	AB01968659		0.41	95.75	7.17
Chloroquine	AB00053436		1.10	111.08	7.50
Remdesivir	AB01952209		4.42	100.27	15.00
Hydroxychloroquine	AB00053257		5.04	93.14	30.00
E64d (Aloxistatin)	AB01955411		16.72	98.55	30.00

Table 3. Cytotoxicity of Clioquinol (CLQ) and Analogues in Vero E6 Cells, in Comparison to Reference Inhibitors of SARS-CoV-2.

Inhibitor ID	Cytotoxicity CC ₅₀ (μM)	Minimum Viability (%)	Concentration at Minimum % Viability (μM)	Maximum Viability (%)	Concentration at Maximum % Viability (μM)
CLBQ14	>30.00	53.50	15.00	107.88	0.12
CLCQ	>30.00	60.82	15.00	101.51	0.06
CLQ	>30.00	61.83	30.00	105.82	0.23
CalpainInhibitorIV	>7.17	98.29	3.59	104.99	0.22
Chloroquine	>30.00	95.63	15.00	106.60	0.06
Remdesivir	>30.00	97.49	3.75	104.49	0.06
Hydroxychloroquine	>30.00	96.88	3.75	103.65	0.06
E64d (Aloxistatin)	>30.00	100.06	15.00	112.76	0.12

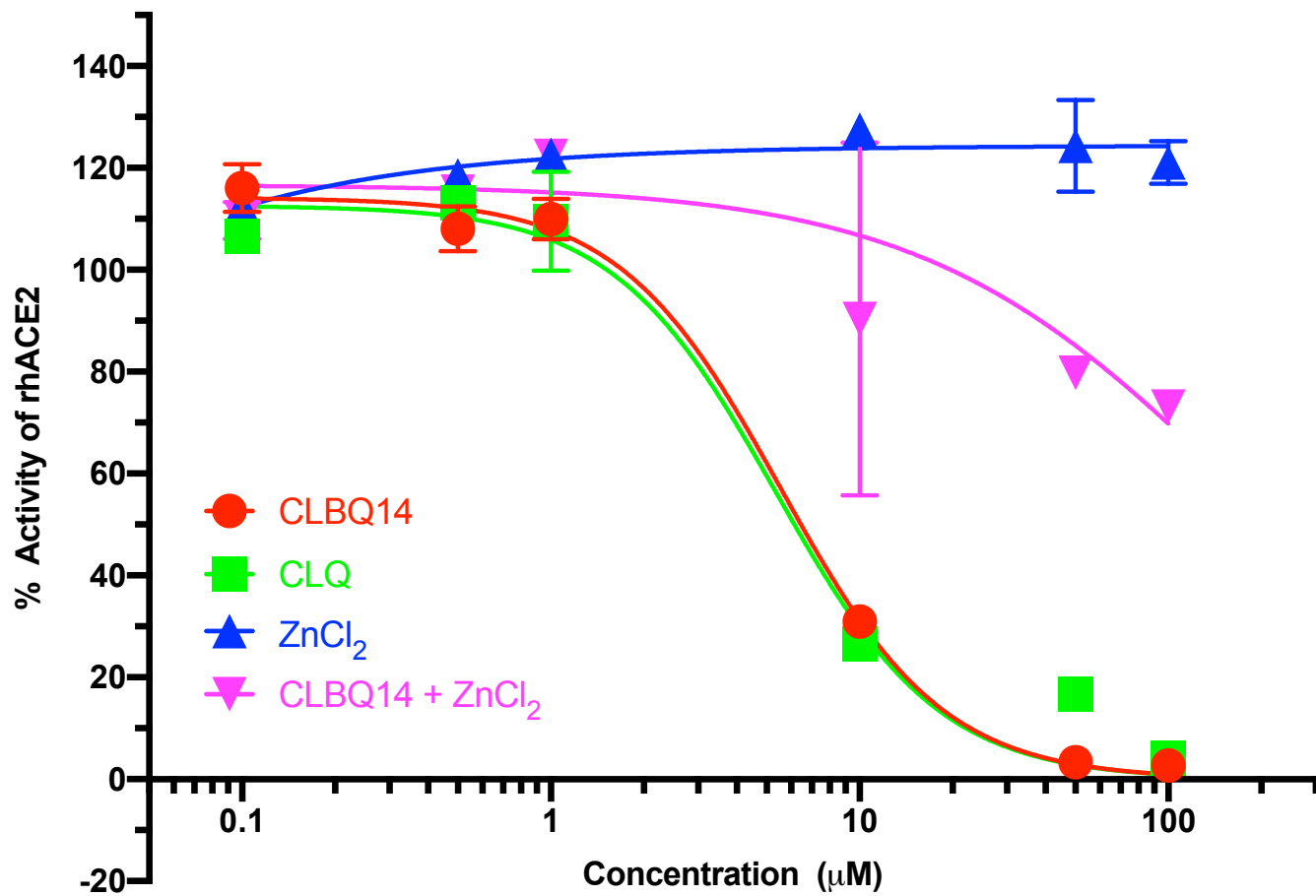


Figure 3. Effect of Clioquinol (CLQ) and Analogues against ACE2 Exopeptidase Activity: A. CLBQ14 (Circles – red), B. CLQ (Squares – green), and C. ZnCl₂ (Triangle – blue), and D. CLBQ14 and ZnCl₂ (Inverted Triangles – magenta).

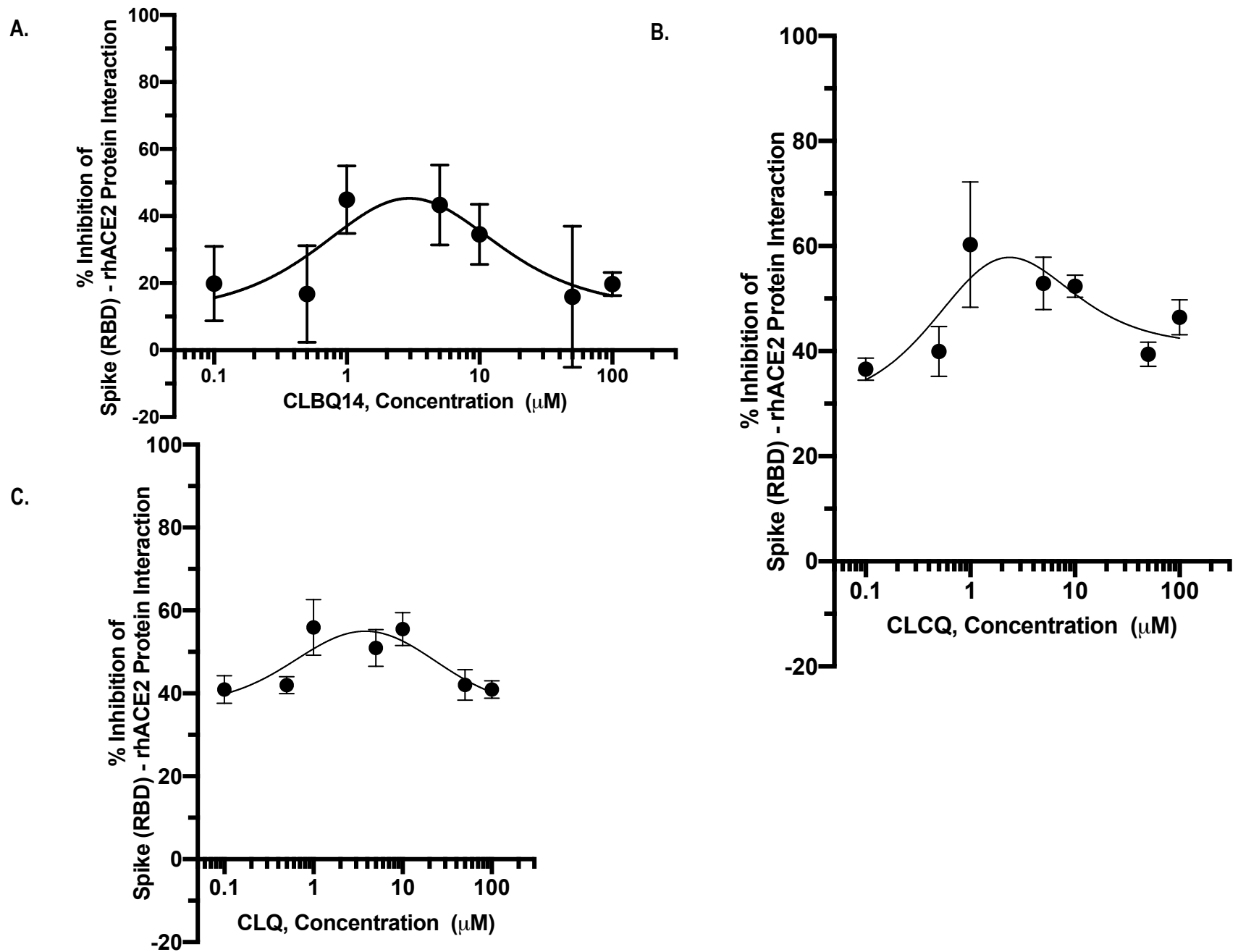


Figure 4. Inhibition of rhACE2 and SARS-CoV-2 Spike (RBD) Protein Interaction by Clioquinol (CLQ) and Analogues: A. CLBQ14, B. CLCQ, and C. CLQ.

Table 4. Activity of Clioquinol (CLQ) and Analogues against ACE2 Exopeptidase Activity and ACE2 and SARS-CoV-2 Spike (RBD) Protein Interaction.

Inhibitor ID	IC ₅₀ (μM)		
	ACE2 Exopeptidase Activity Assay	Spike (RBD)-ACE2 Interaction Assay (IC _{50.1} (μM))	Spike (RBD)-ACE2 Interaction Assay (IC _{50.2} (μM))
CLBQ14	5.55	2.76	3.06
CLCQ	<10	1.74	1.91
CLQ	5.36	0.85	18.15
*CLBQ14 and ZnCl ₂	159.00	ND	ND
* ZnCl ₂	ND	ND	ND

*Higher Concentrations need to be conducted to determine IC₅₀